AD

AD-E403 296

Technical Report ARMET-TR-10004

RECENT COMBINED EFFECTS EXPLOSIVES TECHNOLOGY

E.L. Baker
D. Murphy
D. Suarez
C. Capellos
P. Cook
P. Anderson
E. Wrobel
U.S. Army ARDEC
Picatinny Arsenal, NJ 07806

L. Stiel
Polytechnic University
Brooklyn, NY 11201

July 2010

U.S. ARMY ARMAMENT RESEARCH, DEVELOPMENT AND ENGINEERING CENTER

Munitions Engineering Technology Center

Picatinny Arsenal, New Jersey

The views, opinions, and/or findings contained in this report are those of the author(s) and should not be construed as an official Department of the Army position, policy, or decision, unless so designated by other documentation.

The citation in this report of the names of commercial firms or commercially available products or services does not constitute official endorsement by or approval of the U.S. Government.

Destroy this report when no longer needed by any method that will prevent disclosure of its contents or reconstruction of the document. Do not return to the originator.

REPORT DOCUMENTATION PAGE	Form Approved OMB No. 0704-01-0188

1. REPORT DATE (DD-MM-YYYY)	2. REPORT TYPE	3. DATES COVERED (*From - To*)
July 2010		

4. TITLE AND SUBTITLE

RECENT COMBINED EFFECTS EXPLOSIVES TECHNOLOGY

5a. CONTRACT NUMBER

5b. GRANT NUMBER

5c. PROGRAM ELEMENT NUMBER

6. AUTHORS

E.L. Baker, D. Murphy, D. Suarez, C. Capellos, P. Cook, P. Anderson, and E. Wrobel - U.S. Army ARDEC

L. Stiel - Polytechnic University

5d. PROJECT NUMBER

5e. TASK NUMBER

5f. WORK UNIT NUMBER

7. PERFORMING ORGANIZATION NAME(S) AND ADDRESS(ES)

U.S. Army ARDEC, METC
Energetics, Warheads & Manufacturing Technology Directorate
(RDAR-MEE-W)
Picatinny Arsenal, NJ 07806-5000

Polytechnic University
Brooklyn, NY 11201

8. PERFORMING ORGANIZATION REPORT NUMBER

9. SPONSORING/MONITORING AGENCY NAME(S) AND ADDRESS(ES)

U.S. Army ARDEC, ESIC
Knowledge & Process Management (RDAR-EIK)
Picatinny Arsenal, NJ 07806-5000

10. SPONSOR/MONITOR'S ACRONYM(S)

11. SPONSOR/MONITOR'S REPORT NUMBER(S)

Technical Report ARMET-TR-10004

12. DISTRIBUTION/AVAILABILITY STATEMENT

Approved for public release; distribution is unlimited.

13. SUPPLEMENTARY NOTES

14. ABSTRACT

Eigenvalue detonation theory has been shown to explain the observed behavior of new aluminized combined effects explosives. An analytical cylinder test model has long been used the U.S. Army Armaments Research, Development and Engineering Center, Picatinny Arsenal, New Jersey for explosive equation of state calibration and verification. The analytic model was originally based on adiabatic expansion along the principle isentrope from the Chapman-Jouguet state. The analytic cylinder test model was recently updated to include eigenvalue detonation theory and associated adiabatic expansion from the fully reacted Hugoniot weak point. The results show a small reduction of explosive work output for eigenvalue detonations compared to Chapman-Jouguet detonations. The details of the analytic cylinder test are presented. Additionally, new semi-metal combined explosive compositions based on Si and B were investigated using the JAGUAR thermochemical equation of state and the new eigenvalue extended analytic cylinder model. These new semi-metal based formulations show potential high energy and high blast performance equal or greater than current combined effects explosives and also provide significant promise for reduced sensitivity.

15. SUBJECT TERMS

Eigenvalue detonation theory, Aluminized combined effects explosives, Analytic cylinder test, Adiabatic expansion, Semi-metal combined explosive compositions

16. SECURITY CLASSIFICATION OF:			17. LIMITATION OF ABSTRACT	18. NUMBER OF PAGES	19a. NAME OF RESPONSIBLE PERSON
a. REPORT	b. ABSTRACT	c. THIS PAGE			Dr. Ernest Baker
U	U	U	SAR	19	19b. TELEPHONE NUMBER (Include area code) (973) 724-5079

CONTENTS

	Page
Background	1
Taylor Long Bomb Model	1
Analytic Cylinder Model	4
Cylinder Wall Thinning	6
High Rate Continuum Modeling Comparison	7
Al, Si, and B Based Combined Effects Explosives	9
Eigenvalue Analytic Cylinder Model	10
Conclusions	12
References	13
Distribution List	15

FIGURES

1	Taylor long bomb model	2
2	Analytic cylinder test model	5
3	ALE-3D cylinder test modeling at 10 μs intervals	6
4	TNT analytic model versus ALE-3D modeling	8
5	LX-14 analytic model versus ALE-3D modeling	8
6	PAX-30 cylinder test experimental results comparison to modeling	9
7	Al based combined effects explosive (PAX-30) analytic models versus ALE-3D	11
8	Si based combined effects explosive analytic models versus ALE-3D	11
9	B based combined effects explosive analytic models versus ALE-3D	12

BACKGROUND

The U.S. Army combined effects aluminized explosives (PAX-29, PAX-30, and PAX-42) were previously demonstrated to achieve both excellent metal pushing and high blast energies in both cylinder tests and warhead configurations. The excellent metal pushing capability of these combined effects explosives is due to the earlier exothermic conversion of aluminum to aluminum oxide as compared to traditional blast explosives. However, the traditional Chapman-Jouguet detonation theory does not explain the observed detonation states achieved by these combined effects explosives. The eigenvalue detonation theory explains the observed behavior and was incorporated into the computational design process for warhead configurations (refs. 1 through 3). An analytic cylinder test model has long been used by the U.S. Army Armament Research, Development and Engineering Center (ARDEC), Picatinny Arsenal, New Jersey for explosive equation of state calibration and verification. This analytic model has been shown to provide close agreement to high rate continuum modeling. However, the analytic model was based on adiabatic expansion along the principle isentrope from the Chapman-Jouguet state. As it has been hypothesized that the current combined effects explosives expand from a weak point on the fully reacted Hugoniot, the validity of the analytic cylinder test comes into question for these explosives. The analytic cylinder test model was recently updated to include the eigenvalue detonation theory and associated adiabatic expansion from the fully reacted Hugoniot weak point.

TAYLOR LONG BOMB MODEL

Gurney formulation is a traditional analytic method used for high explosive material acceleration modeling (ref. 4). The work of Taylor (ref. 5) provides the framework for a more fundamental methodology for modeling exploding cylinders, including axial flow effects. Based on the assumption of heavy confinement, Taylor proposed the use of Reynolds hydraulic treatment and isentropic detonation products flow to model a heavy long cylindrical bomb expansion. The model is very similar to the Delaval nozzle theory (ref. 6), but includes the momentum of the cylinder wall. A diagram of a Taylor heavy long cylinder expansion due to high explosive detonation is presented in figure 1. It should be noted that flow velocities are relative to the detonation velocity, D. Using the Jones-Wilkens-Lee-Baker [JWLB (ref. 7)] thermo-dynamic equation of state, the Taylor heavy long cylindrical bomb model can be represented as follows.

Mass:

$$\rho_0 D r_0^2 = \rho U r^2 \tag{1}$$

Linear Momentum:

$$2\pi r P = mD\frac{d\Theta}{dt} \tag{2}$$

Energy:

$$\rho_0 D r_0^2 \left(\frac{D^2}{2} + e_0\right) = \rho U r^2 \left(\frac{U^2}{2} + e\right) + P U r^2 \tag{3}$$

Principle isentrope:

$$P = \sum_i A_i e^{-\frac{R_i \rho_0}{\rho}} + C\left(\frac{\rho_0}{\rho}\right)^{-(\omega+1)} \tag{4}$$

$$de = -Pd\left(\frac{1}{\rho}\right) \tag{5}$$

Taylor angle:

$$v = 2Dsin\frac{\Theta}{2} \tag{6}$$

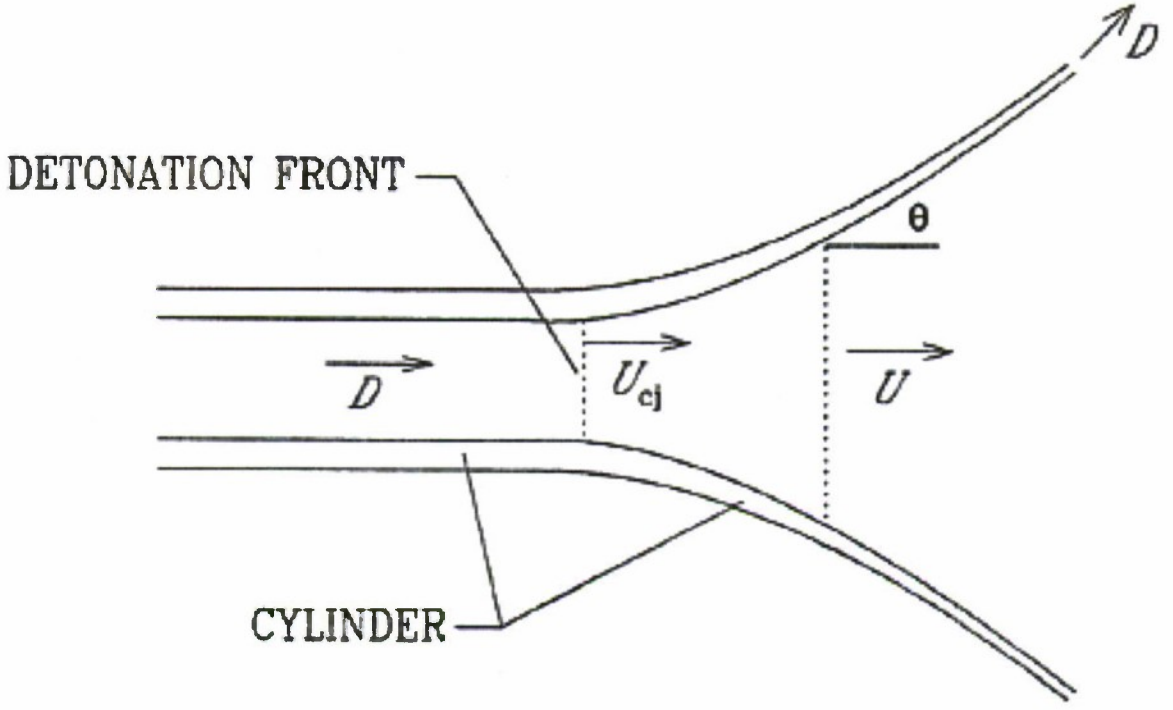

Figure 1
Taylor long bomb model

Based on the assumption of heavy confinement, this model neglects radial flow effects in the detonation products. Additionally, the detonation products flow is assumed to be isentropic from the Chapman-Jouguet state and cylinder strength is neglected. To achieve an easier computational form, the following reduction is made.

$$c \equiv \rho_0 \pi r_0^2 \tag{7}$$

$$(1) \Rightarrow \left(\frac{r}{r_0}\right)^2 = \frac{\rho_0 D}{\rho} \tag{8}$$

$$v_r \equiv \frac{dr}{dt} = Dsin\Theta, (2) \Longrightarrow 2\pi rP = -mD^2 \frac{dcos\Theta}{dr} = mD^2 2\frac{dsin^2\frac{\Theta}{2}}{dr} \tag{9}$$

$$(6) \Longrightarrow \frac{d\frac{v^2}{2}}{dr} = \frac{2\pi r}{M} P \Longrightarrow d\frac{v^2}{2} = \frac{c}{m}\frac{P}{\rho_0} d\left(\frac{r}{r_o}\right)^2$$

$$= \frac{c}{m} d\left[\frac{P}{\rho_0}\left(\frac{r}{r_0}\right)^2\right] - \frac{c}{m}\left(\frac{r}{r_0}\right)^2 \frac{1}{\rho_0} dP \tag{10}$$

$$(8) \Rightarrow d\frac{v^2}{2} = \frac{c}{m} D\left[d\left(\frac{P}{\rho U}\right) - \frac{1}{\rho U} dP\right] \tag{11}$$

$$(3) \Rightarrow \frac{D^2}{2} + e_0 = \frac{U_{cj}^2}{2} + \frac{P_{cj}}{\rho_{cj}} + e_{cj} = \frac{U^2}{2} + \frac{P}{\rho} + e \tag{12}$$

$$\Rightarrow \frac{U^2}{2} - \frac{U_{cj}^2}{2} = -\left(\frac{P}{\rho} - \frac{P_{cj}}{\rho_{cj}}\right) - \left(e - e_{cj}\right) \tag{13}$$

$$(5) \Rightarrow de = -Pd\left(\frac{1}{\rho}\right), (13) \Rightarrow d\frac{U^2}{2} = -d\frac{P}{\rho} + Pd\frac{1}{\rho} = -\frac{1}{\rho}\, dP \tag{14}$$

$$\Rightarrow -\frac{1}{\rho U} dp = dU, (7) \Rightarrow d\frac{v^2}{2} = \frac{c}{m} D\left[d\left(\frac{P}{\rho U}\right) + dU\right] \tag{15}$$

$$\Rightarrow \frac{V^2}{2} = \frac{c}{m} D\left(\frac{P}{\rho U} - \frac{P_{cj}}{P_{cj} U_{cj}} + U - U_{cj}\right) \tag{16}$$

$$P_{cj} = \rho_o D\left(D - U_{cj}\right) = \rho_{cj} U_{cj}\left(D - U_{cj}\right) \tag{17}$$

$$(16) \Rightarrow \frac{v^2}{2} = \frac{c}{m} D\left[\frac{P}{\rho U} - (D - U)\right] \tag{18}$$

The final form is as follows

$$P = \sum_i A_i e^{-\frac{R_i \rho_0}{\rho}} + C\left(\frac{\rho_0}{\rho}\right)^{-(\omega+1)} \tag{19}$$

$$e_{cj} - e = \sum_i \frac{A_i}{\rho_0 R_i}\left(e^{-\frac{R_i \rho_0}{\rho_{cj}}} - e^{-\frac{R_i \rho_0}{\rho}}\right) + \frac{C}{\omega \rho_0}\left[\left(\frac{\rho_0}{\rho_{cj}}\right)^{-\omega} - \left(\frac{\rho_0}{\rho}\right)^{-\omega}\right] \tag{20}$$

$$\frac{U^2}{2} = \frac{U_{cj}^2}{2} + \frac{P_{cj}}{\rho_{cj}} - \frac{P}{\rho} + \left(e_{cj} - e\right) \tag{21}$$

$$\frac{V^2}{2} = \frac{c}{m} D\left[\frac{P}{\rho U} - (D - U)\right] \tag{22}$$

$$\rho = \frac{\rho_o D}{\left(\frac{r}{r_0}\right)^2} \tag{23}$$

In our implementation, the set of equations is solved for a given area expansion, $(r/r_0)^2$ using Brent's method (ref. 8).

ANALYTIC CYLINDER MODEL

Building upon Taylor's long bomb model, one method of including radial flow effects is to assume spherical surfaces of constant thermodynamic properties and mass flow in the detonation products (ref. 9). The detonation products mass flow is assumed to be in a perpendicular direction to the spherical surfaces. A diagram of a products constant spherical surfaces cylinder expansion due to high explosive detonation is presented in figure 2. Again, it should be noted that flow velocities are relative to the detonation velocity, D. If constant detonation product properties are assumed across spherical surfaces, the following model results.

Mass:

$$\rho_{cj} U_{cj} A_0 = \rho U A \tag{24}$$

Axial momentum:

$$P_{cj} r_0^2 - P r^2 = \frac{m}{\pi} D^2 cos\Theta - \frac{m}{\pi} D^2 + \rho U^2 r^2 - \rho_{cj} U_{cj}^2 r_0^2 \tag{25}$$

Energy:

$$\rho_{cj} U_{cj} A_0 \left(\frac{U_{cj}^2}{2} + e_{cj}\right) + P_{cj} U_{cj} A_0 = \rho U A \left(\frac{U^2}{2} + e\right) + PUA \tag{26}$$

Principle isentrope:

$$P = \sum_i A_i e^{-\frac{R_i \rho_0}{\rho}} + C\left(\frac{\rho_0}{\rho}\right)^{-(\omega+1)}, \mathrm{de} = -\mathrm{Pd}\left(\frac{1}{\rho}\right) \tag{27}$$

Taylor angle:

$$v = 2D sin\frac{\Theta}{2} \tag{28}$$

Spherical area:

$$A = \pi r^2 \frac{2(1-cos\Theta)}{\sin^2\Theta} \tag{29}$$

To achieve an easier computational form, the following reduction is made

$$(28) \Rightarrow \cos\Theta = 1 - 2\sin^2\frac{\Theta}{2} = 1 - 2\left(\frac{v}{2D}\right)^2 = 1 - \frac{\left(\frac{v}{D}\right)^2}{2} \tag{30}$$

$$(29), (30) \Rightarrow A = 2\pi r^2 \frac{\frac{(v/D)^2}{2}}{1-\left[1-\frac{\left(\frac{v}{D}\right)^2}{2}\right]^2} = \frac{\pi r^2}{1-\left(\frac{v}{2D}\right)^2} \tag{31}$$

$$(24), (31) \Rightarrow \rho = \frac{\rho_{cj} U_{cj} \pi r_0^2}{U \pi r^2}\left[1 - \left(\frac{v}{2D}\right)^2\right] = \frac{\rho_{cj} U_{cj}}{U\left(\frac{r}{r_0}\right)^2}\left[1 - \left(\frac{v}{2D}\right)^2\right] \tag{32}$$

$$(25) \Rightarrow P_{cj}r_0^2 - Pr^2 = -\frac{m}{\pi}D^2\frac{\left(\frac{v}{D}\right)^2}{2} - \rho_{cj}U_{cj}^2 r_0^2 + \rho U^2 r^2 \tag{33}$$

$$\Longrightarrow \frac{v^2}{2} = \left[P\left(\frac{r}{r_0}\right)^2 - P_{cj} + \rho\left(\frac{r}{r_0}\right)^2 U^2 - \rho_{cj}U_{cj}^2\right]\frac{C}{m\rho_0} \tag{34}$$

$$(26) \Rightarrow \frac{U_{cj}^2}{2} + e_{cj} + \frac{P_{cj}}{\rho_{cj}} = \frac{U^2}{2} + e + \frac{P}{\rho} \tag{35}$$

$$\Rightarrow \frac{U^2}{2} = \frac{U_{cj}^2}{2} + e_{cj} + \frac{P_{cj}}{\rho_{cj}} - e - \frac{P}{\rho} \tag{36}$$

The final form is as follows

$$(27) \Rightarrow P = \sum_i A_i e^{\frac{-R_i\rho_0}{\rho}} + C\left(\frac{\rho_0}{\rho}\right)^{-(\omega+1)} \tag{37}$$

$$(27) \Rightarrow e_{cj} - e = \sum_i \frac{A_i}{\rho_0 R_i}\left(e^{\frac{-R_i\rho_0}{\rho_{cj}}} - e^{\frac{-R_i\rho_0}{\rho}}\right) + \frac{C}{\omega\rho_0}\left[\left(\frac{\rho_0}{\rho_{cj}}\right)^{-\omega} - \left(\frac{\rho_0}{\rho}\right)^{-\omega}\right] \tag{38}$$

$$(36) \Rightarrow \frac{U^2}{2} = \frac{U_{cj}^2}{2} + \frac{P_{cj}}{\rho_{cj}} - \frac{P}{\rho} + e_{cj} - e \tag{39}$$

$$(34) \Longrightarrow \frac{v^2}{2} = \left[P\left(\frac{r}{r_0}\right)^2 - P_{cj} + \rho\left(\frac{r}{r_0}\right)^2 U^2 - \rho_{cj}U_{cj}^2\right]\frac{C}{m\rho_0} \tag{40}$$

$$(32) \Rightarrow \rho = \frac{\rho_{cj}U_{cj}}{U\left(\frac{r}{r_0}\right)^2}\left[1 - \left(\frac{v}{2D}\right)^2\right] \tag{41}$$

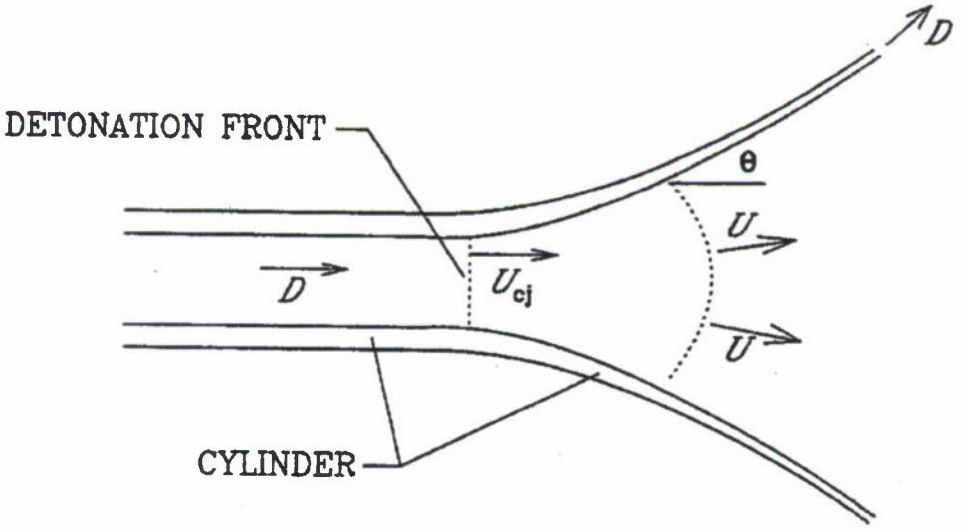

Figure 2
Analytic cylinder test model

Again, in our implementation, the set of equations is solved for a given area expansion, $(r/r_0)^2$, using Brent's method. The Taylor long bomb model is appropriate for large charge to mass ratio configurations, where the radial momentum associated with the detonation products is relatively small. However, the spherical surface approach has been shown to be much more accurate for smaller mass to charge ratios without any loss of agreement at larger mass to charge ratios (ref. 9). It should be recognized that this analytic modeling approach neglects initial acceleration due to shock processes (ref. 10) and is therefore anticipated to be more accurate as the initial shock process is damped out.

CYLINDER WALL THINNING

The analytic cylinder models (fig. 2), as expressed, do not consider the fact that the cylinders thin during radial expansion. One simple way to account for this wall thinning is to assume that the wall cross-sectional area remains constant and r and v represents the inside radius and inside surface wall velocity.

$$v_{out} = v\frac{r_{in}}{r_{out}} \;,\; r_{out}^2 = r_{in}^2 + r_{0out}^2 - r_{0in}^2 \tag{42}$$

HIGH RATE CONTINUUM MODELING COMPARISON

ALE-3D (fig. 3) high rate continuum modeling was compared to analytic cylinder test modeling using identical JWLB equations of state for TNT and LX-14. The JWLB equations of state were parameterized using JAGUAR thermochemical equation of state modeling (ref. 11). Table 1 presents the TNT and LX-14 JWLB parameters. The 1.2 in. outer diameter, 1 in. inner diameter, 10 in. long copper cylinder was modeled using the Johnson-Cook material model. Figures 4 and 5 present the comparison of the analytic cylinder test model to the ALE-3D modeling for TNT and LX-14, respectively. The analytic cylinder model slightly under predicts the velocities at two and three inside area expansions, but is in very close agreement by six and seven inside area expansions. This is consistent with the fact that this analytic modeling approach neglects initial acceleration due to shock processes. Strong shock effects are typically observed in the two to three volume expansion region and are pretty much damped out by the six volume expansions, where very close agreement between the analytic model and ALE-3D results are observed.

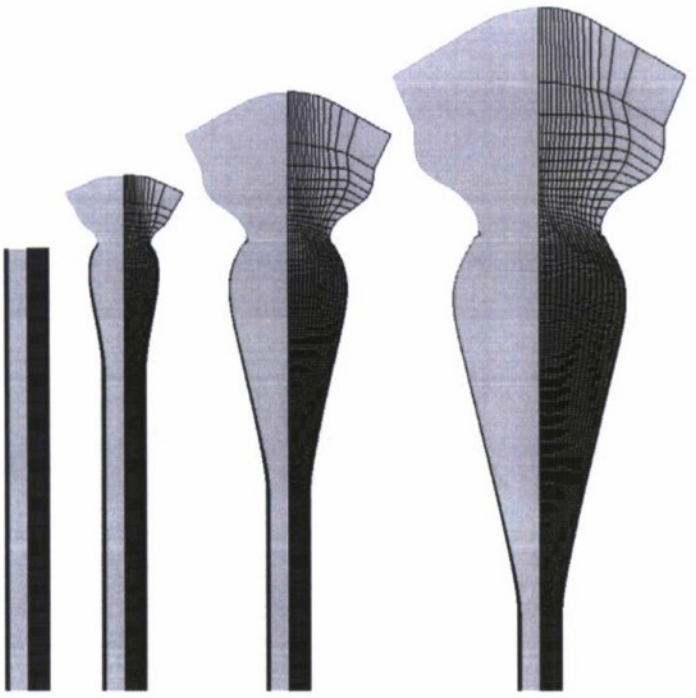

Figure 3
ALE-3D cylinder test modeling at 10 μs intervals

Table 1
JWLB parameters for various explosives

	TNT	LX-14	PAX-30	PAX-30Si	PAX-30B
Density (g/cm^3)	1.6300	1.8350	1.9090	1.8890	1.8690
E0 (Mbar)	0.0657	0.1032	0.1376	0.1358	0.1441
D (cm/s)	0.6817	0.8691	0.8429*	0.8095*	0.8584*
P (Mbar)	0.1930	0.3418	0.2464*	0.2601*	0.2395*
A1 (Mbar)	399.2140	399.1910	405.3810	598.5830	584.5750
A2 (Mbar)	56.2911	52.1951	14.8887	71.6056	0.0130
A3 (Mbar)	0.8986	1.59892	1.49138	1.3717	1.7536
A4 (Mbar)	0.0092	0.0249	0.0076	0.0045	0.0126
R1	28.0876	27.4041	13.2982	25.2998	12.5850
R2	9.7325	8.4331	8.0204	9.9478	59.7687
R3	2.5309	2.6293	2.4942	2.3865	2.6542
R4	6.9817	0.7498	0.3566	0.3112	0.4086
AI1	58.2649	68.6476	66.6542	0.0028	0.9895
AI2	6.1981	6.7497	5.7776	13.0069	2.3314
BI1	2.9036	4.1338	3.1440	3091.9200	0.9997
BI2	-3.2455	-4.4607	-3.2552	-10.0596	-0.8634
RI1	25.5601	26.2448	25.5996	12.3214	21.5439
RI2	1.7034	1.6977	1.7099	2.0342	1.2931

* Eigenvalue weak point detonation state (not the Chapman-Jouguet state)

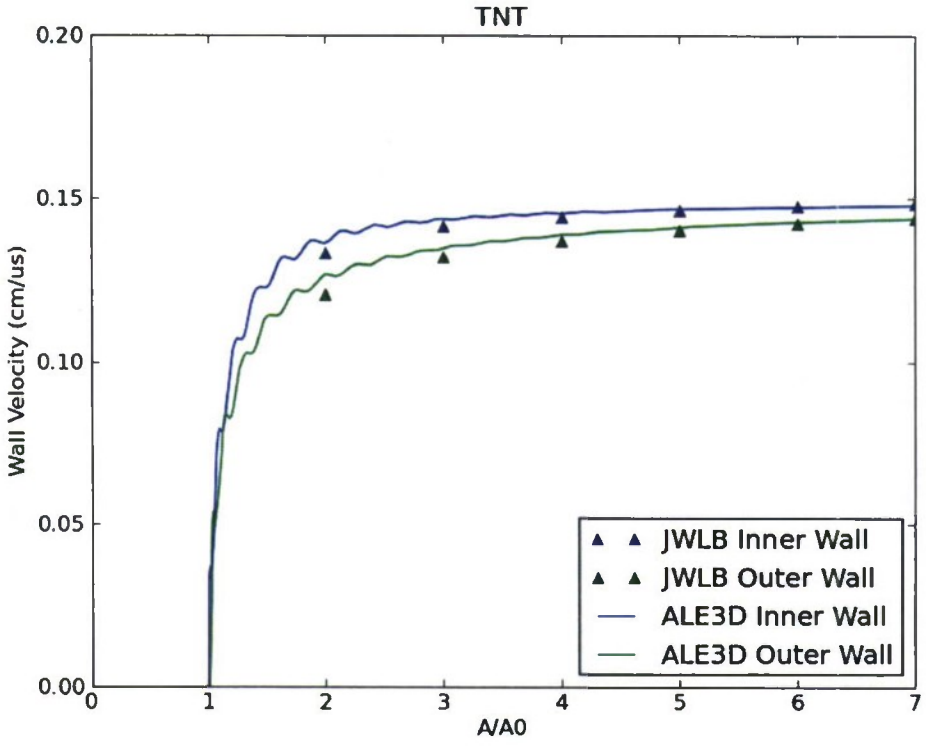

Figure 4
TNT Analytic model versus ALE3D modeling

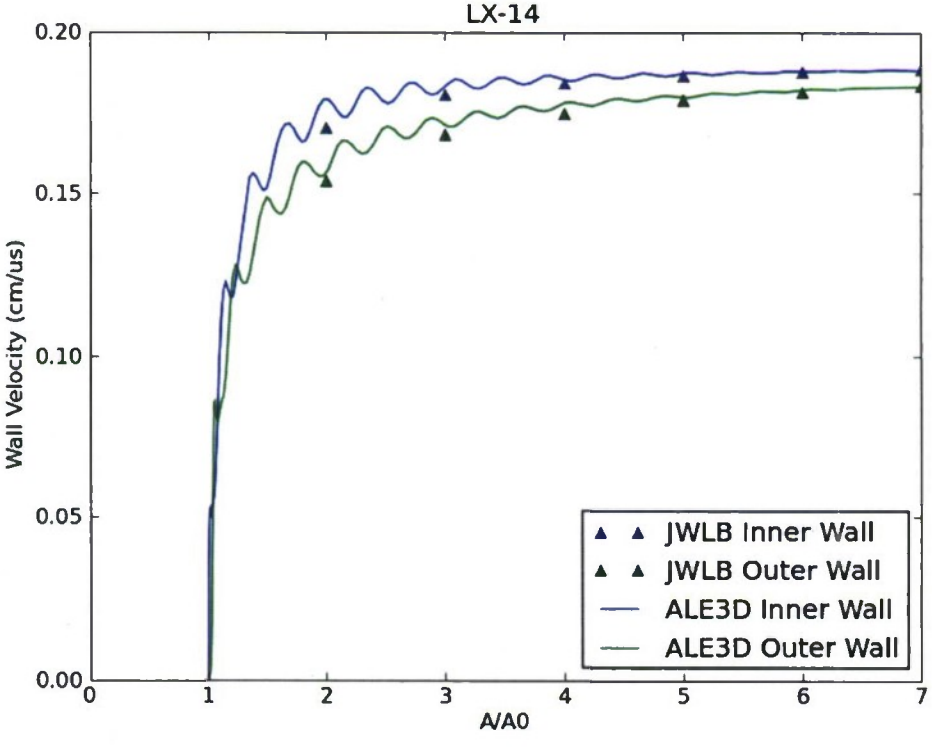

Figure 5
LX-14 Analytic model versus ALE3D modeling

ALUMINUM (Al), SILICON (Si), AND BARON (B) BASED COMBINED EFFECTS EXPLOSIVES

The combined effects aluminized explosives PAX-29, PAX-30, and PAX-42 were previously demonstrated to achieve both excellent metal pushing and high blast energies in both cylinder test and warhead configurations. Modeling comparisons using JAGUAR predicted JWLB parameters to cylinder test experiments were previously completed with very good agreement. Figure 6 presents the PAX-30 results. More recently, new semi-metal combined explosive compositions based on Si and B were investigated using the JAGUAR thermo-chemical equation of state. As part of this investigation, improved modeling of Si, B, and their possible detonation products was completed using non-linear optimization to parameterize with available Hugoniot data, diamond anvil data, and melt curves (refs. 12 and 13). These new semi-metal based formulations show potential high energy and high blast performance equal or greater than current combined effects explosives and also provide significant promise for reduced sensitivity. Although B has seen some investigation as an additive for increased performance (refs. 14 and 15), Si has not been investigated for increased performance. B has a relatively high melt temperature (2300°C) compared to Si (1400°C) and Al (660°C), which could inhibit its ability to participate in a detonation reaction. However, the melt temperature of Si drops considerably with pressure and is passivated with a much thinner oxide layer than aluminum. For this reason, Si is actually predicted to have shorter characteristic melt times than Al at a given particle size. For this reason, Si is expected to participate in a detonation reaction at larger particle sizes compared to Al, which could provide reduced sensitivity. Eigenvalue detonation theory was previously shown to explain the observed behavior of the PAX-29, PAX-30, and PAX-42 aluminized combined effects explosives and is indicated for Si and B based combined effects explosives as well.

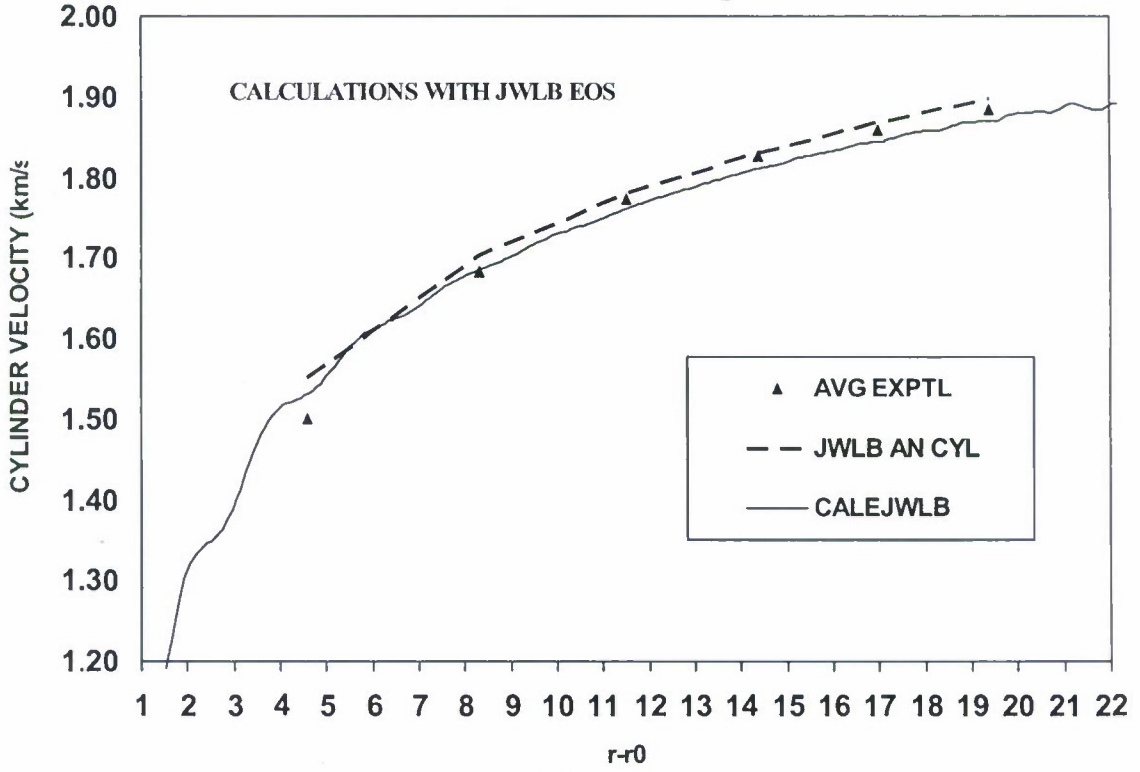

Figure 6
PAX-30 cylinder test experimental results comparison to modeling

EIGENVALUE ANALYTIC CYLINDER MODEL

Eigenvalue detonation theory is observed for aluminized combined effects explosives and is anticipated for Si and B based combined effects explosive. For this reason, it was of interest to develop a modified analytic cylinder test model that would provide a description of the detonation products isentropic expansion from the eigenvalue detonation weak point, rather than from the Chapman-Jouguet state. The JWLB thermodynamic equation of state is essentially developed around a principle isentrope fit. It was found that the most straightforward method of implementation of an eigenvalue detonation analytic cylinder model was to refit the isentrope associated with the eigenvalue weak point using the equation 27 form. In this way, equations 24 through 43 remain correct, except that the eigenvalue weak point is used, rather than the Chapman-Jouguet state. With this approach, it is important to realize that the weak-point isentrope fit is not the same as the principle isentrope fit. The final form is as follows

$$P = \sum_i A_{wi} e^{\frac{-R_{wi}\rho_0}{\rho}} + C_w \left(\frac{\rho_0}{\rho}\right)^{-(\omega+1)} \tag{43}$$

$$e_w - e = \sum_i \frac{A_{wi}}{\rho_0 R_{wi}} \left(e^{\frac{-R_{wi}\rho_0}{\rho_w}} - e^{\frac{-R_{wi}\rho_0}{\rho}} \right) + \frac{C_w}{\omega \rho_0} \left[\left(\frac{\rho_0}{\rho_w}\right)^{-\omega} - \left(\frac{\rho_0}{\rho}\right)^{-\omega} \right] \tag{44}$$

$$\frac{U^2}{2} = \frac{U_w^2}{2} + \frac{P_w}{\rho_w} - \frac{P}{\rho} + e_w - e \tag{45}$$

$$\frac{v^2}{2} = \left[P \left(\frac{r}{r_0}\right)^2 - P_w + \rho \left(\frac{r}{r_0}\right)^2 U^2 - \rho_w U_w^2 \right] \frac{c}{m\rho_0} \tag{46}$$

$$\rho = \frac{\rho_w U_w}{U\left(\frac{r}{r_0}\right)^2} \left[1 - \left(\frac{v}{2D_w}\right)^2 \right] \tag{47}$$

Figures 7 through 9 compare predicted cylinder test results using the eigenvalue analytic cylinder test model for Al, Si, and B based combined effects explosives. Excellent agreement between the analytic cylinder test model and ALE-3D cylinder test modeling is achieved. The compositions are HMX based with 15% Al (PAX-30), 15% Si, and 10% B. Table 1 presents the JAGUAR derived JWLB parameters used in ALE-3D for the Al (PAX-30), Si (PAX-30Si), and B (PAX-30B) based compositions. The JWLB and eigenvalue detonation weak point isentrope equation 43 was parameterized using JAGUAR thermochemical predicted behavior. The results for these explosives show only a very small reduction of explosive work output for eigenvalue detonations compared to Chapman-Jouguet detonations. This is due to the fact that the Chapman-Jouguet principle isentrope and eigenvalue weak point isentrope lie very close to each other. Both the Si and B are predicted to have similar or increased performance over LX-14, similar to the Al based PAX-30, which has been experimentally demonstrated.

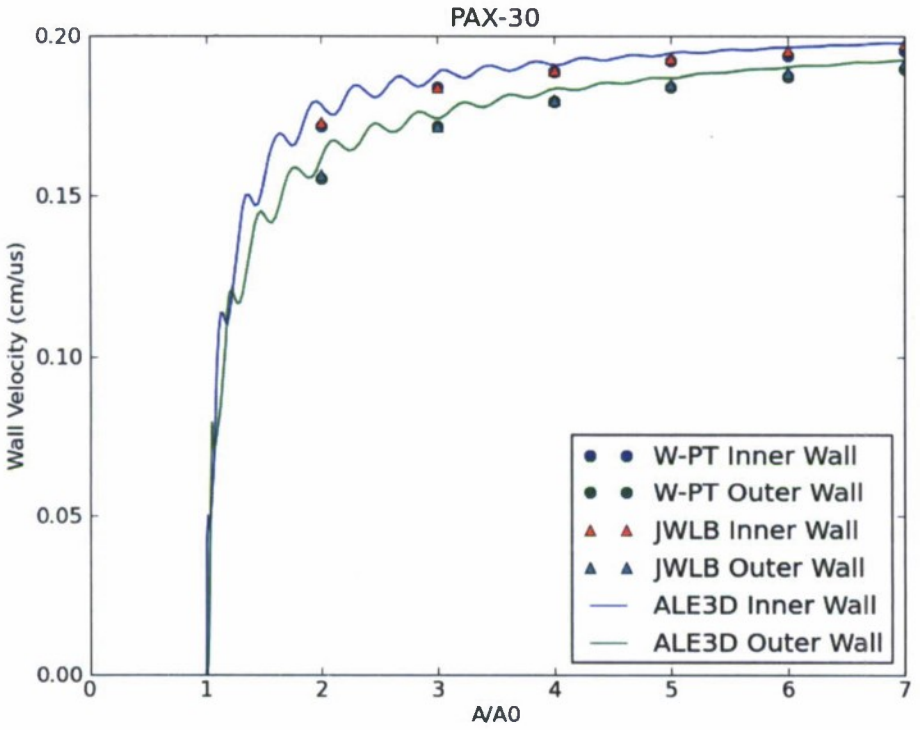

Figure 7
Al based combined effects explosive (PAX-30) analytic models versus ALE-3D

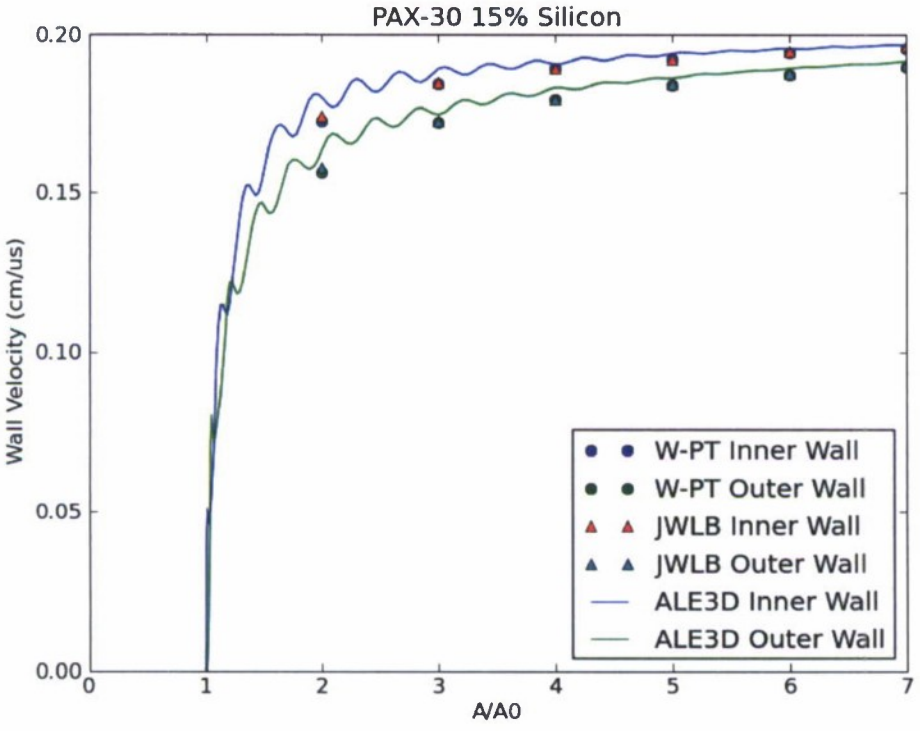

Figure 8
Si based combined effects explosive analytic models versus ALE-3D

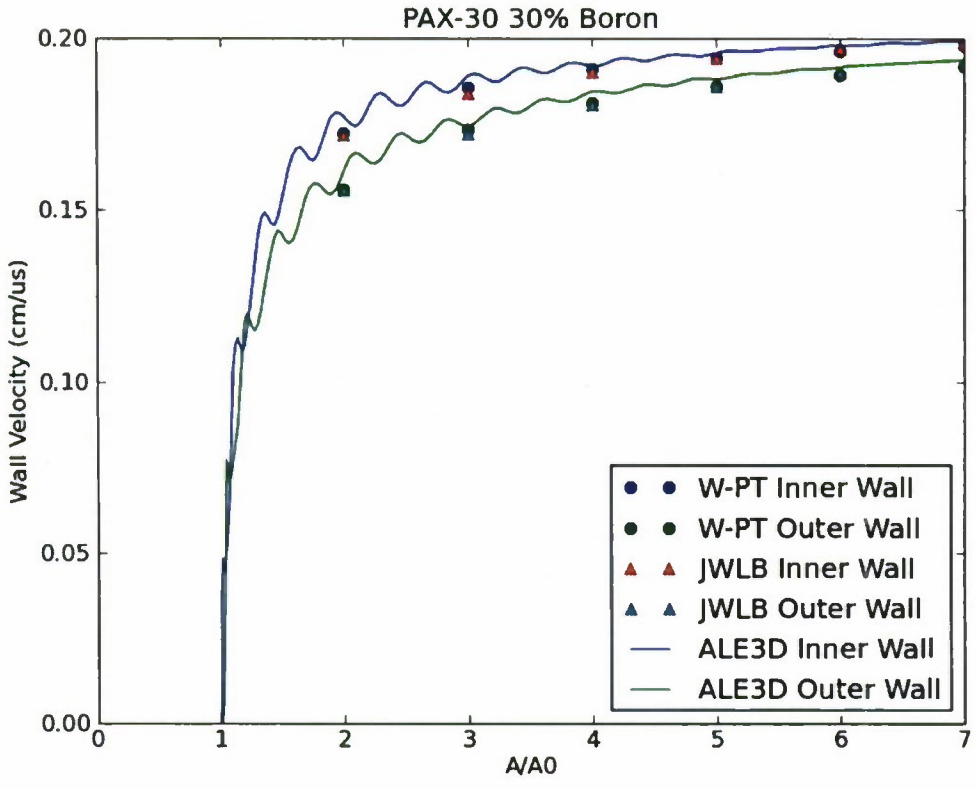

Figure 9
B based combined effects explosive analytic models versus ALE-3D

CONCLUSIONS

A new eigenvalue extended analytic cylinder expansion model was developed based around isentropic expansion from the detonation eigenvalue weak point, rather than from the Chapman-Jouguet state. Semi-metal combined explosive compositions based on silicone (Si) and boron (B) was investigated using the JAGUAR thermochemical equation of state and this new eigenvalue analytic cylinder expansion model. The results for these explosives show only a very small reduction of explosive work output for eigenvalue detonations compared to Chapman-Jouguet detonations. This is due to the fact that the Chapman-Jouguet principle isentrope and eigenvalue weak point isentrope lie very close to each other. These new semi-metal based formulations show potential high energy and high blast performance equal or greater than current aluminized combined effects explosives and may also provide significant promise for reduced sensitivity. In particular, due to the relatively small predicted characteristic melt times, the Si based explosive may provide high work output at early volume expansions using larger particle sizes. The use of larger particle size may provide a reduction in sensitivity. In contrast, the high melt temperature of B may inhibit its ability to participate in a detonation reaction, so that predicted increase in early work output may not be achievable.

REFERENCES

1. Baker, E.L.; Stiel, L.I.; Capellos, C.; Balas, W.; and Pincay, J., "Combined Effects Aluminized Explosives," Proceedings of the International Ballistics Symposium, New Orleans, LA, 22-26 September 2008.

2. Balas, W.; Daniels, A.; Baker, E.L.; Capellos, C.; Vuong, T.; and Stiel, L.I.; "Recent Development and Application of Combined Effects Explosives," Proceedings of the 2008 1^{1th} Joint Classified Bombs, Warheads & Ballistics Symposium, Monterey, CA 11-14 February 2008.

3. Baker, E.L.; Capellos, C.; and Stiel, L.I., "Theory and Detonation Products Equations of State for a New Generation of Combined Effects Explosives," 7th Joint Classified Bombs/Warheads & Ballistics Symposium, Monterey, CA, 9-12 August 2004.

4. Gurney, R. W., "The Initial Velocities of Fragments from Bombs, Shells, and Grenades," BRL Report 405, U.S. Army Ballistic Research Laboratory, Aberdeen Proving Ground, MD, 1943.

5. Taylor, G. I., "Analysis of the Explosion of a Long Cylindrical Bomb Detonated at One End," Scientific Papers of Sir G. I. Taylor, Vol 111:2770286, Cambridge University Press (1963), 1941.

6. Courant, R. and Friedrichs, K., "Supersonic Flow and Shock Waves," Interscience Publishers, New York, 1984.

7. Baker, E.L., "An Explosives Products Thermodynamic Equation of State Appropriate for Material Acceleration and Overdriven Detonation: Theoretical Background and Formulation," Technical Report ARAED-TR-91 013, U.S. Army Armament Research, Development and Engineering Center, Picatinny Arsenal, NJ, 1991.

8. Brent, R., Algorithms for Minimization without Derivatives, Prentice-Hall, Englewood Cliffs, NJ, 1973. Reprinted by Dover Publications, Mineola, New York, January 2002.

9. Baker, E.L., "Modeling and Optimization of Shaped Charge Liner Collapse and Jet Formation," Technical Report ARAED-TR-92017, U.S. Army Armament Research, Development and Engineering Center, Picatinny Arsenal, NJ, January 1993.

10. Backofen, J.E., "Modeling a Material's Instantaneous Velocity during Acceleration Driven by a Detonation's Gas-Push," 2005: Proceedings of the Conference of the American Physical Society Topical Group on Shock Compression of Condensed Matter, AIP Conf. Proc., Volume 845, pp. 936-939, 28 July 2006.

11. Stiel, L.I. and Baker, E.L., "Detonation Energies of Explosives by Optimized JCZ3 Procedures," Proceedings of the APS Topical Conference on Shock Compression of Condensed Matter, New Hampton, MA, August 1997.

12. Stiel, L.I.; Baker, E.L.; Capellos, C. and Poulos, W., "JAGUAR Procedures for Detonation Behavior of Silicon Containing Explosives," Proceedings of the 15th APS Topical Conference on Shock Compression of Condensed Matter, Kohala Coast, Hawaii, 24-29 June 2007.

13. Stiel, L.I.; Baker, E.L. and Capellos, C., "JAGUAR Procedures for Detonation Behavior of Explosives Containing Boron," Proceedings of the 16th APS Topical Conference on Shock Compression of Condensed Matter, Nashville, TN, 29 June -3 July 2009.

14. Arnold, W. and Rottenkolber, E., "The Performance of Insensitive Blast Enhanced Explosives," 2009 Insensitive Munitions & Energetic Materials Technology Symposium, Tucson, AZ, May 11-14, 2009.

15. Sezaki, T.; Datea, S.; and Satoh, J., "Study on the Effects of Addition of Boron Particles to RDX-Based PBX Regarding Prevention of Neumann Effect," Materials Science Forum Vols. 465-466, pp 195-200, 2004.

DISTRIBUTION LIST

U.S. Army ARDEC
ATTN: RDAR-EIK
RDAR-GC
RDAR-MEE-W, E. Baker
Picatinny Arsenal, NJ 07806-5000

Defense Technical Information Center (DTIC)
ATTN: Accessions Division
8725 John J. Kingman Road, Ste 0944
Fort Belvoir, VA 22060-6218

Commander
Soldier and Biological/Chemical Command
ATTN: AMSSB-CII, Library
Aberdeen Proving Ground, MD 21010-5423

Director
U.S. Army Research Laboratory
ATTN: AMSRL-CI-LP, Technical Library
Bldg. 4600
Aberdeen Proving Ground, MD 21005-5066

Chief
Benet Weapons Laboratory, WSEC
U.S. Army Research, Development and Engineering Command
Armament Research, Development and Engineering Center
ATTN: RDAR-WSB
Watervliet, NY 12189-5000

Director
U.S. Army TRADOC Analysis Center-WSMR
ATTN: ATRC-WSS-R
White Sands Missile Range, NM 88002

Chemical Propulsion Information Agency
ATTN: Accessions
10630 Little Patuxent Parkway, Suite 202
Columbia, MD 21044-3204

GIDEP Operations Center
P.O. Box 8000
Corona, CA 91718-8000